

Geometrothermodynamics of interface domain structures in phase transitions on 5-dimensional contact statistical manifold with pseudo-Finsler metric

H. V. Grushevskaya, N. G. Krylova, G. G. Krylov, V. Balan

Abstract. Geometrothermodynamics of interface domains emerging in first-order phase transitions modeled on a 5-dimensional statistical contact manifold is proposed in entropy representation. The supporting structure is given by a space-time regarded a hypersurface embedded in the tangent space, and its signature is provided by the Hessian of a pseudo-Finsler-type Lagrangian. A many-relaxation-time evolution of domains (nuclei) is represented a set of sections of the indicatrix surface in the tangent space at different pseudo-times. Within the phase-transition space-time, whose Finsler-metric signature is $(- - -)$, we say that such a section - obtained from sectioning the indicatrix by a plane transversal to pseudo-time axis - lives in the physically meaningful region of the space-time, and its geodesics are associated with a stable state of the domain structure. If the indicatrix section evolves from the physically meaningful region into a region with alternating-sign metric signature, this testifies that the domain structure associated with the geodesic loses its stability and becomes a metastable one.

M.S.C. 2010: 53B40, 53C60.

Key words: pseudo-Finsler metric, signature, indicatrix, curvature tensor, geometrothermodynamics, Langmuir monolayer, first-order phase transition.

1 Introduction

To date, the development of modern electronic devices based on quasi-two-dimensional crystal monomolecular layers (monolayers) is a topical issue. Therefore, studies of phase transitions from two-dimensional (2D) gas into 2D crystal that proceed on an interface are high-promising and subject of notable interest within condensed matter physics. Domain structures can be visualized in the 2D phase transition of first order, in contrast to three-dimensional (3D) 1st-order phase transitions [30]. For the first-order phase transition from expanded 2D-liquid to 2D liquid-crystal state in Langmuir monolayers, the interface interactions and the presence of domains with a range of relaxation times reveal themselves in compression isotherms (dependencies of

surface pressure π upon the area per molecule A_s) as a gently sloping area (plateau) testifying a metastable monolayer state. The plateau is non-horizontal one in contrast to horizontal plateau observed in the case of 3D 1st-order phase transitions [21, 31, 32, 2, 16]. An additional feature of the 2D phase transitions is the dependence of the phase transition dynamics on compression rate [31, 11, 22, 13, 18, 16]. It has been shown [31, 19, 2, 6, 18] that the distribution of domain relaxation times and interface interactions - such as electrocapillary forces - acting on the interphase boundary air/aqueous subphase should be taken into account, to correctly describe the kinetic characteristic of the 2D phase transitions. Electrocapillary forces disrupt the hydrate complexes of amphiphilic molecules that form the 2D gaseous phase of the Langmuir monolayer. The compressed monolayer of amphiphilic molecules which are "ejected" from the hydrate complexes, is crystalized. This monolayer - separated from the subphase and called Langmuir–Blodgett monolayer - can be transferred to the solid substrate. Due to the promising applications of nanostructured Langmuir–Blodgett films in nanoelectronics and biosensorics, the development of new phase-transition models is a strong concern. Generally accepted kinetic models are based on Johnson–Mehl–Avrami–Kolmogorov model of fast nucleation processes, with subsequent slow growth of phase domain (nuclei) [3, 17]. These models are suitable for describing the homogenous phase transition, without account of long range correlations scaling domain structure. However the metastable domains, scaled both in time and space, reveal themselves as certain glass-like transient-phase along with the slow and the fast processes [23]. Second order response functions, like the compressibility, change their sign at least twice during the first-order phase transition with distribution of relaxation times.

To date, geometrical approaches are widely used to model many physical problems in cosmology, quantum mechanics and condensed matter physics. The advantage of geometrical models is the possibility to apply well-developed mathematical theory of topological invariants to the description and analysis of physical processes. Geometrothermodynamic models of phase transition developed in literature [33, 34, 29, 26] are in good agreement with the second-order phase transitions only. The known geometrothermodynamic 1st-order-phase-transition models of Van der Waals type [8] predict that theoretical second-order response functions change the sign once, which contradicts experimental observations.

The Weyl curvature tensor measures the curvature of a pseudo-Riemannian manifold. In General Relativity Theory, the Weyl curvature governs the propagation of gravitational waves through regions of space devoid of matter. If the Weyl tensor vanishes in dimension more than 3, then the metric is locally conformally flat [24]. A Weyl-type curvature tensor is one of the important projective invariants of a Finsler space. A Finsler space is of scalar flag curvature if and only if its Weyl tensor identically vanishes [1]. In the paper [9], it was proven that the Weyl-type curvature tensor W_j^i can be defined in a way able to characterize Finsler metrics of constant curvature. The Weyl-type curvature tensor, constructed as:

$$W_j^i = R_j^i - \frac{1}{n-1} R_l^l \delta_j^i + \frac{1}{2(n-1)} \frac{\partial R_l^l}{\partial y^j} y^i,$$

coincides with the projective Weyl tensor if and only if the Finsler metric is of constant curvature. Here R_j^i is the Ricci curvature tensor, y^i are velocities, n is the space

dimension, here and in what follows the summation is assumed over repeated indexes. If the Weyl curvature for Finsler metrics (Randers-type metrics) does not depend on the velocity [35], i.e.,

$$W_i^j = R_i^j - \frac{R_l^l}{n-1} \delta_i^j,$$

then it reduces to the classical projective Weyl tensor from the Riemannian context.

Thus, in spite of the rapidly growing amount of theoretical results devoted to the phase transitions of first order, the description of the emerging domain structure still remains a challenge. Moreover, a realistic analytical description of domain kinetics of first-order phase transitions, is absent.

We proposed a pseudo-Finsler geometrothermodynamic model of the first-order phase transition in Langmuir monolayers in [14]. In [6] a statistical contact manifold of the 1st-order phase transition on interface has been constructed as a space of probability distributions p_i , $i = 1, \dots, N$, $N \rightarrow \infty$ for the configurations $\{\vec{r}_1, t_1; \dots; \vec{r}_{i-1}, t_{i-1}; \vec{r}_i, t_i + \Delta t_i; \vec{r}_{i+1}, t_{i+1}; \dots; \vec{r}_N, t_N\}$ of the monolayer, at a point \vec{r}_i , $i = 1, \dots, N$ where at the moment $t_i + \Delta t_i$, a nucleus with lifetime τ_i , $i = 1, \dots, N$, $N \rightarrow \infty$, is produced. An action, whose physical meaning is entropy production for this manifold, determines the geodesics of the thermodynamic phase space-time $\{\vec{r}, t, \vec{r}, \dot{\xi}\}$, with the velocity defined by the derivatives $\dot{\vec{r}} = \frac{d\vec{r}}{ds}$, $\dot{\xi} = \frac{dt}{ds} \equiv \frac{d\xi}{ds}$ relative to an evolution parameter s . The relaxation time (lifetime) of domain (nucleus) is determined by the rate of time evolution $\dot{\xi}$. It has been demonstrated that singular behavior of the scalar Berwald curvature B_c of the thermodynamic phase space corresponds to divergence of matter thermodynamic quantities, such as compressibility during the 1st-order phase transition [4, 6, 7, 18]. The scaling behavior of the scalar curvature in the phase transition was proven in [6]. At that, $B_c(s)$ changes its sign at least twice during the first-order phase transition with distribution of relaxation times [5, 15]. We demonstrated that the first-order phase transitions proceed along with signature change events. A pseudo-Finsler metric dl_F has been chosen as a metric of a hypersurface $\dot{\xi} = const$, assuming that the time flows at a constant rate and does not stop: $\dot{\xi} \neq 0$. In this paper, we analyze the signature structure of the contact statistical manifold which is endowed with a pseudo-Finsler metric, generalized over whole manifold.

Our goal is to investigate the effects of signature change events in geometrothermodynamics of interface domain structures, based on the behavior of the projective curvature Weyl and Douglas tensors of the generalized pseudo-Finsler metrics.

2 First-order phase transition geometrothermodynamics

The Lagrangian of the Langmuir monolayer reads [14, 6]

$$(2.1) \quad L = \frac{1}{2}m \left(\frac{dr}{dt}\right)^2 + \frac{1}{2}mr^2 \left(\frac{d\varphi}{dt}\right)^2 + U(r, t) - p|V|r^5 e^{\frac{2t|V|}{r}} \frac{dt}{dr},$$

where the potential of electrocapillary forces $U(r, t)$ is

$$U(t, r) = p \left\{ \left[-\frac{4}{3}r^5 + \frac{16}{15}(|V|t)r^4 + \frac{1}{30}(|V|t)^2 r^3 + \frac{1}{45}(|V|t)^3 r^2 + \frac{1}{45}(|V|t)^4 r + \frac{2}{45}(|V|t)^5 \right] e^{\frac{2|V|t}{r}} - \frac{4}{45} \frac{(|V|t)^6}{r} \text{Ei} \left(\frac{2|V|t}{r} \right) \right\}.$$

Then, the parameterized action of the contact statistical manifold has the form:

$$(2.2) \quad dl_F(d\vec{r}, dt) = mc^2 \dot{\xi} ds - L(s) \dot{\xi} ds = \left(A \frac{\dot{\xi}^2}{\dot{r}} + B \dot{\xi} - C \frac{(\dot{r}^2 + r^2 \dot{\varphi}^2)}{2\dot{\xi}} \right) ds.$$

Here the parameters A , B , C are given by

$$(2.3) \quad \begin{aligned} A &= p |V| r^5 e^{\frac{2|V|t}{r}}, \\ B &= mc^2 - p \left(\left(-\frac{4}{3} r^5 + \frac{16}{15} (|V|t) r^4 + \frac{1}{30} (|V|t)^2 r^3 + \frac{1}{45} (|V|t)^3 r^2 + \frac{1}{45} (|V|t)^4 r \right. \right. \\ &\quad \left. \left. + \frac{2}{45} (|V|t)^5 \right) e^{\frac{2|V|t}{r}} - \frac{4}{45} \frac{(|V|t)^6}{r} \text{Ei} \left[\frac{2|V|t}{r} \right] \right), \\ C &= m, \quad p = \frac{\pi^2 q^2}{\varepsilon \varepsilon_0} \frac{\rho_0^2}{R_0^2}, \quad \dot{r} = \frac{x\dot{x} + y\dot{y}}{r}, \end{aligned}$$

where $\text{Ei} \left[\frac{2|V|t}{r} \right]$ is the special function *exponential integral*, m is the proper particle mass, V is the monolayer-compression rate, p is a monolayer constant, which includes molecular charge q , the initial surface density ρ_0 of the molecules, and the initial monolayer radius R_0 ; as well, r and φ are polar coordinates of the monolayer. The pseudo-time t is the time of phase transition, whose flow is defined by the distribution of times of relaxation processes in the monolayer. Also, $\dot{\xi}$, \dot{r} and $\dot{\varphi}$ define the corresponding derivatives of t , r and φ , respectively, relative to the evolution parameter s ; at that, $\dot{\xi}$ determines the relaxation time (lifetime) of the nucleus. The action (2.2) of the contact Finsler–Lagrangian statistical manifold describes the entropy of the two-dimensional (2D) monolayer [6]. The action dl_F (2.2) has the meaning of entropy production. The action (2.2) defines the metric on the contact statistical manifold endowed with the metric function

$$(2.4) \quad \mathcal{L} = -dl_F^2(\dot{r}, \dot{\xi}) = - \left(A \frac{\dot{\xi}^2}{\dot{r}} + B \dot{\xi} - \frac{C}{2} \frac{(\dot{r}^2 + r^2 \dot{\varphi}^2)}{\dot{\xi}} \right)^2.$$

The sign "minus" is chosen by virtue of the Second Law of Thermodynamics, and the stability of the system in free energy representation requires that the Hessian is a negative-definite symmetric tensor field, which infers maximal entropy. Since dl_F (2.2) is a homogeneous function of degree 1 with respect to velocities, the defined thermodynamic space is pseudo-Finslerian [28, 27].

The dynamics of the system is determined by the Euler-Lagrange equations:

$$(2.5) \quad \frac{dy^i}{ds} + 2G^{(i)} = 0, \quad \frac{dx^k}{ds} = \dot{x}^k \equiv y^k,$$

where the spray components G^i are

$$G^i(y) = \frac{1}{4} g^{il}(y) \left\{ 2 \frac{\partial g_{jl}}{\partial x^k}(y) - \frac{\partial g_{jk}}{\partial x^l}(y) \right\} y^j y^k,$$

and the metric tensor g_{ij} is given by the expression

$$(2.6) \quad g_{ij} = \frac{1}{2} \frac{\partial^2 \mathcal{L}}{\partial y^i \partial y^j},$$

where

$$y_1 = \dot{\xi}, \quad y_2 = \dot{r}, \quad y_3 = \dot{\varphi}.$$

In explicit form, $\{g_{ij}\}$ is written as:

$$(2.7) \quad \begin{aligned} g_{11} &= -\frac{\dot{\xi}^4 \left(6A^2\dot{\xi}^2 + 6AB\dot{\xi}\dot{r} + B^2\dot{r}^2 \right) + 3C^2 \left(r^2\dot{r}\dot{\varphi}^2 + \dot{r}^3 \right)^2}{\dot{\xi}^4\dot{r}^2}, \\ g_{12} = g_{21} &= -\frac{-A\dot{\xi}^5(4A\dot{\xi} + 3B\dot{r}) + AC\dot{\xi}^3\dot{r} \left(r^2\dot{\varphi}^2 - \dot{r}^2 \right) - 4C^2 \left(r^2\dot{r}^4\dot{\varphi}^2 + \dot{r}^6 \right)}{\dot{\xi}^3\dot{r}^3}, \\ g_{13} = g_{31} &= \frac{2Cr^2\dot{\varphi} \left(A\dot{\xi}^3 + 2C \left(r^2\dot{r}\dot{\varphi}^2 + \dot{r}^3 \right) \right)}{\dot{\xi}^3\dot{r}}, \\ g_{22} &= -\frac{-2C\dot{\xi}^2\dot{r} \left(A\dot{\xi}r^2\dot{\varphi}^2 + B\dot{r}^3 \right) + A\dot{\xi}^5(3A\dot{\xi} + 2B\dot{r}) + 2C^2 \left(r^2\dot{r}^4\dot{\varphi}^2 + 3\dot{r}^6 \right)}{\dot{\xi}^2\dot{r}^4}, \\ g_{23} = g_{32} &= -\frac{2Cr^2\dot{\varphi} \left(A\dot{\xi}^3 + 2C\dot{r}^3 \right)}{\dot{\xi}^2\dot{r}^2}, \\ g_{33} &= -\frac{2Cr^2 \left(C \left(3r^2\dot{r}\dot{\varphi}^2 + \dot{r}^3 \right) - \dot{\xi}^2(A\dot{\xi} + B\dot{r}) \right)}{\dot{\xi}^2\dot{r}} \end{aligned}$$

The equations (2.5) are complicated and can be solved only numerically. The initial conditions are chosen as follows: $\dot{\xi}(s=0) = 1$ and $\dot{r}(s=0) = \dot{r}_0$. These conditions mean that the evolution of the macroscopic system is considered starting from the production of a first critical nucleus, which leaves the hydrate complex having the velocity \dot{r}_0 . Besides, one has in mind that the nucleus relaxation time (life-time) $\dot{\xi}$ is small enough not to rapidly combine with other nuclei to produce a large thermodynamically stable phase region. The numerical simulation results of analysis of the equations (2.5) for the geodesics, are shown in fig. 1.

As one can see from fig. 1a–d, the equations (2.5) describe the transition process, during which the system evolves up to some constant values of t , r , φ . From the physical point of view, the system transits from free motion of molecules in the monolayer of 2D-liquid state, to limit-circle trajectories characterized as for stable states of a 2D-crystal.

To analyze the dependence of the radial coordinate r on the evolution parameter s (fig. 1g), we find the relation between the surface pressure increment π_t at the time moment t (provided by a hydrate complex decay and crystalline-phase nucleus production in the metastable state of the monolayer) and the parameter s . In the approximation of weak-interacting nuclei, we can utilize the two-dimensional equation of state for an ideal gas

$$(2.8) \quad \pi_t A_M = N_t k_B T,$$

where A_M is a monolayer area, N_t is an increment of nuclei number at the time moment t , T is a temperature, and k_B is the Boltzmann constant. Since the nuclei number N_t is inverse proportional to relaxation time $\tau = \frac{\Delta t}{\Delta s}$ and since $\pi_t A_M = S_t T$

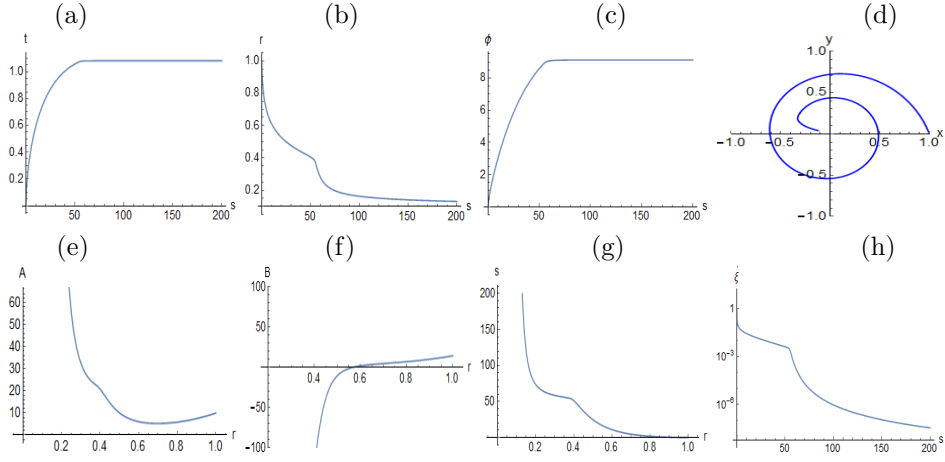


Figure 1: (a)–(d) Geodesics curves $t(s)$, $r(s)$, $\phi(s)$ and geodesic trajectory; (e)–(f) The dependencies of the metric parameters A and B on r along the geodesic; (g)–(h) compression isotherm $s(r)$ and the dependence of relaxation times $\xi(s)$ on the evolution parameter s . The following values of parameters were used: $p = 10$, $m = c = 1$, $V = 1$, $R_0 = 1000$.

due to the first law of thermodynamics, using (2.8) one gets

$$(2.9) \quad \Delta s \sim S_t$$

and hence

$$(2.10) \quad \Delta s \sim \Delta \pi.$$

Here $S_t T$ is the quantity of heat which is gained at the entropy increase S_t . According to the expression (2.10), the dependence $s(r)$ shown in fig. 1g is an isotherm for the phase transition. As one can see, at the values $r \sim 0.4$ the announced plateau is revealed as a characteristic feature of the first-order phase transition.

In fig. 1h, the dependence of relaxation times ξ of hydrate complexes on the evolution parameter s is illustrated. As one can see, during the system evolution, the relaxation times of hydrate complexes decrease. The results of numerical simulation of the dependencies of the metric-function parameters A and B on the radial coordinate r along the geodesics, are shown in fig. 1e,f. As one can see, the value A is always positive during the phase transition. Meanwhile, the initially positive parameter B decreases along the geodesic, and in the vicinity $r \sim 0.6$, it changes the sign. We further show that this leads to a change of signature of the phase transition configuration space.

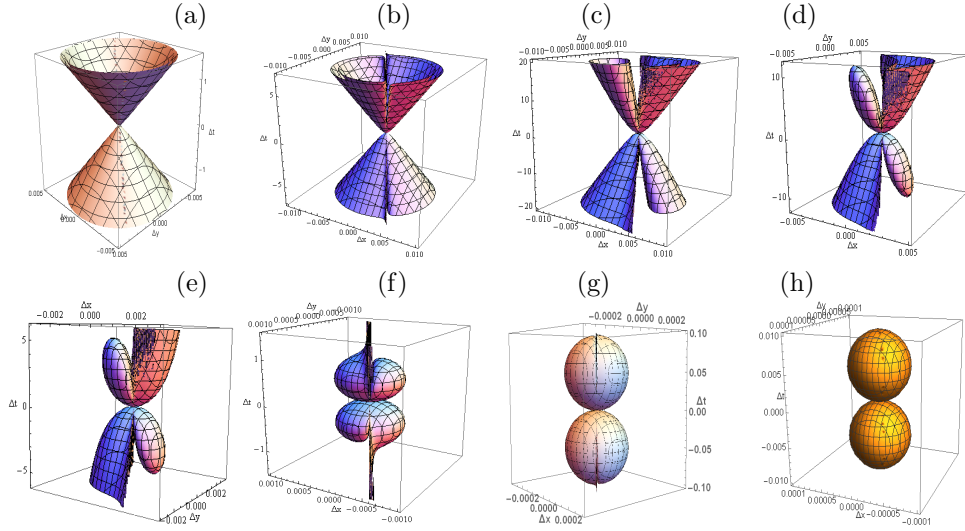


Figure 2: "Spacelike" indicatrices of pseudo-Finsler space at $A = 10^{-5}$, $C = 10^6$, $r = 0.1$ and different B : $B = 10$ (a), 1 (b), 0.1 (c), 10^{-15} (d), -0.1 (e), -1 (f), -10 (g), $B = -100$ (h)

3 Riemann-Finsler structures in the monolayer configuration space

Let us investigate the structures emerging in the contact statistical manifold with the metric (2.4). At a point $x_0 = \{x_0^i\}$ from M , the indicatrix I_{x_0} is formed by the ends of the unit tangent vectors [10, 28, 20, 25, 12], and it is described by the equation $F(x_0^i, y^i) = 1$. The indicatrix is a hypersurface in the tangent space $T_{x_0}M$, which characterizes the metric of Finsler space, depending on direction [28]. A section of the indicatrix with a plane $\Delta t = const$ - is transversal to the pseudo-time axis - is in the physically meaningful region of the phase space of local space-time signature $(- -)$, and the geodesics are trajectories associated with stable states of the domain. Let, at

Table 1: The Hessian signatures of different space regions

Region	Sign Δ_1	Sign Δ_2	Sign Δ_3	Hessian signature (n_+, n_-)
I	-	-	+	(1,2)
II	-	+	+	(1,2)
III	-	-	-	(2,1)
IV	-	+	-	(0,3)
V	+	-	-	(2,1)
VI	+	-	+	(1,2)

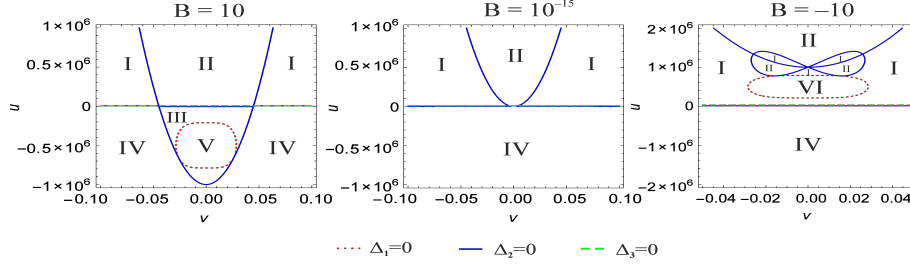


Figure 3: Separating of the (u, v) space regions with different signatures by contour plots $\Delta_i = 0$, $i = 1, 2, 3$. The regions I, ..., VI with different signatures are presented in Table 1. Dependencies corresponding to $\Delta_1 = 0$ (red dotted curve), $\Delta_2 = 0$ (blue solid curve), $\Delta_3 = 0$ (green dashed curve) are calculated at $B = 10$, $B = 10^{-15}$, and $B = -10$; $A = 10^{-5}$, $c = 10^6$, $r = 0.1$.

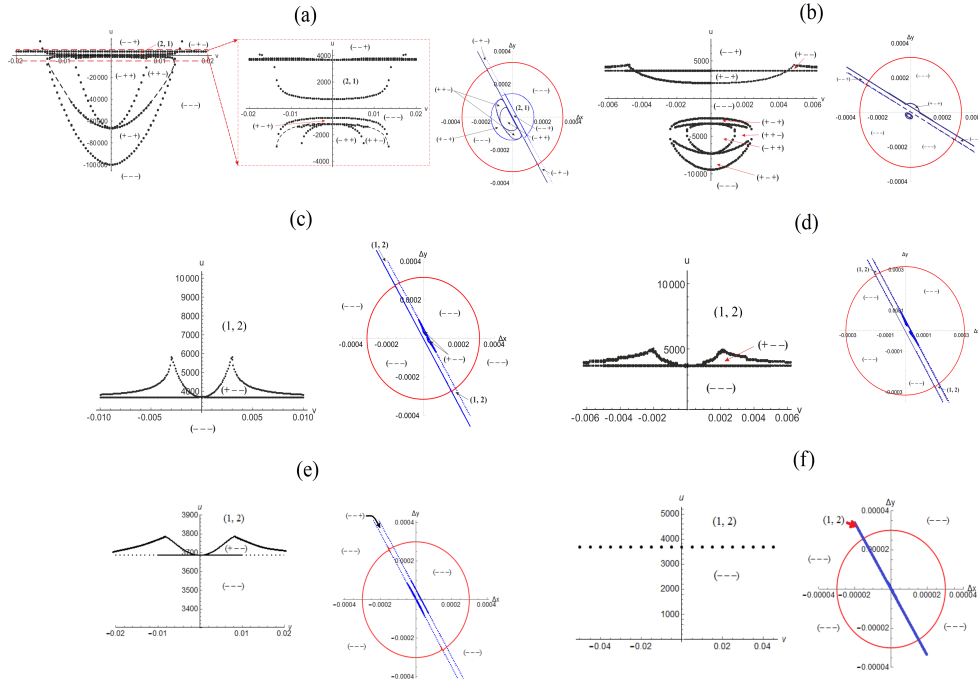


Figure 4: The (u, v) space regions with different metric signature (left) and indicatrix projections (red curve) in the tangent space $(\Delta x, \Delta y)$ (right) at small values of Δt . (a) $B = 1$, $\Delta t = 0.1$; (b) $B = 0.1$, $\Delta t = 0.1$; (c) $B = 10^{-15}$, $\Delta t = 0.1$; (d) $B = -0.1$, $\Delta t = 0.1$; (e) $B = -1$, $\Delta t = 0.1$; (f) $B = -100$, $\Delta t = 0.001$. Blue curves separate space regions with different signature. $A = 10^{-5}$.

the moment $\Delta t = C_M$, the indicatrix section evolves from the physically meaningful region towards a region of the phase space with alternating-sign metric signature. Then the domain state associated with this geodesic loses its stability and becomes a metastable domain. Thus, a set of sections of the indicatrix at different pseudo-times Δt presents an evolution of the domain (nucleus), emerging in the first-order phase transition. We shall further study the evolutions of such type.

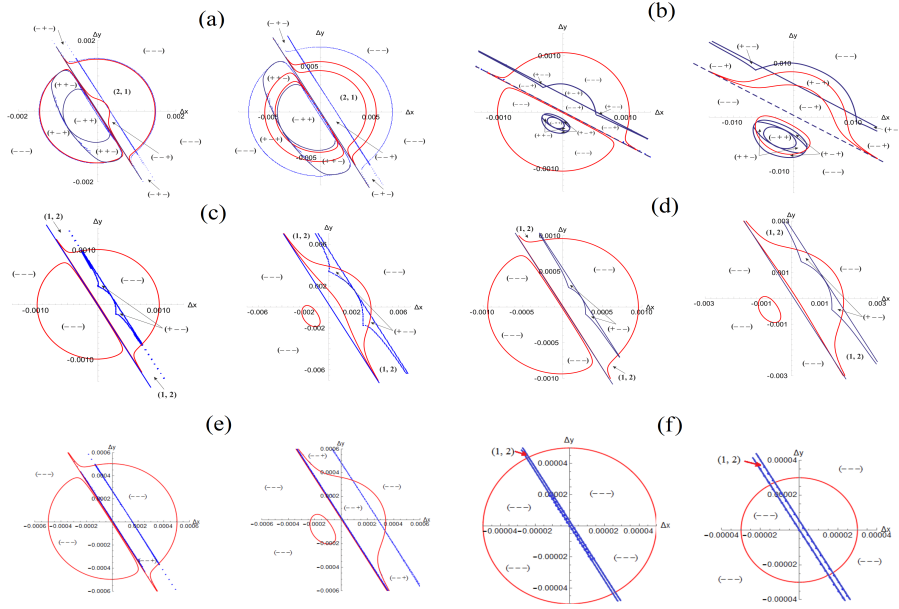


Figure 5: Indicatrix projections (red curves) in the tangent space $(\Delta x, \Delta y)$ at different Δt . (a) $B = 1$, $\Delta t = 1$ (left) and 5 (right) ; (b) $B = 0.1$, $\Delta t = 1$ (left) and 20 (right); (c) $B = 10^{-15}$, $\Delta t = 1$ (left) and 10 (right); (d) $B = -0.1$, $\Delta t = 1$ (left) and 5 (right);(e) $B = -1$, $\Delta t = 0.5$ (left) and 0.9 (right);(f) $B = -100$, $\Delta t = 0.005$ (left) and 0.009 (right). Blue curves separate space regions with different signature. $A = 10^{-5}$.

Our metric function (2.4) is a pseudo-Finsler one, because it takes negative values that there are pseudo-indicatrices defined as

$$(3.1) \quad \mathcal{L}(x_0^i, y^i) = -1$$

accordingly, similar to spacelike intervals from General Relativity Theory. Then, the quadratic equation

$$\left(A \frac{\dot{\xi}^2}{\dot{r}} + B \dot{\xi} - \frac{C}{2} \frac{(\dot{r}^2 + r^2 \dot{\varphi}^2)}{\dot{\xi}} \right)^2 = 1$$

defines two hypersurfaces

$$A \frac{\dot{\xi}^2}{\dot{r}} + B \dot{\xi} - \frac{C}{2} \frac{(\dot{r}^2 + r^2 \dot{\varphi}^2)}{\dot{\xi}} = \pm 1.$$

The Finsler function of the monolayer gives different indicatrix classes, depending on the values of the metric parameters. Let us analyze the shapes of the indicatrix of the metric function (2.4). Fig. 2 shows the results of numerical simulations of "spacelike" indicatrices, depending on the metric parameter B . As one can see from the expressions for the metric function parameters (2.3), when the rate V of the monolayer compression tends to zero, the coefficient A tends to zero as well, and at $B > 0$ the pseudo-Finsler indicatrix degenerates into

$$B\dot{\xi} - \frac{C}{2} \frac{(\dot{r}^2 + r^2\dot{\varphi}^2)}{\dot{\xi}} = \pm 1.$$

Multiplying this expression with $\dot{\xi}$ and completing the perfect square, we get

$$B \left(\dot{\xi} \pm \frac{1}{2B} \right)^2 - \frac{C}{2} (\dot{r}^2 + r^2\dot{\varphi}^2) = \frac{1}{4B}.$$

This defines the indicatrix in the form of a two double-sheeted hyperboloid, shifted to $\pm 1/2B$ along the axis $\dot{\xi}$. The plane $\dot{\xi} = 0$ should be punctured from the indicatrices. For enough large values of the positive parameter $B \rightarrow \infty$, the terms $1/2B$ and $1/4B$ can be neglected and the indicatrix takes a form of a "light cone"

$$B\dot{\xi}^2 - \frac{C}{2} (\dot{r}^2 + r^2\dot{\varphi}^2) = 0,$$

as fig. 2a shows. In this case the velocity-direction distribution is isotropic, due to the axial symmetry of the indicatrix.

At non-zero A , there exist values of the parameter B , for which the shape of the spacelike indicatrix dramatically changes as figs. 2b–h demonstrate. At very small positive B , for example $B = 10^{-15}$ (fig. 2d), or negative B , for example $B = -0.1, -1, -10, -100$ (figs. 2e–h), there are indicatrix sheets which live in closed space-time regions. In this case, the velocities are limited, both in amplitude and direction. From physical point of view, free particles transit into a bounded state. For large negative values of the parameter B , such that $-B \gg A$ and the term $A\dot{\xi}^2/\dot{r}$ is negligible, the indicatrix has a form of two spheres with radius $1/2B$, whose centers are shifted along the axes $\dot{\xi}$ to $\pm 1/2B$, as depicted in fig.2h. The equation describing this case is

$$\left(\dot{\xi} \mp \frac{1}{2|B|} \right)^2 + \frac{C}{2|B|} (\dot{r}^2 + r^2\dot{\varphi}^2) = \frac{1}{4|B|^2}.$$

The minors of the metric tensor (2.7) equal

$$(3.2) \quad \Delta_1 = -\frac{3}{2}(2Au + B)^2 - \frac{3C^2(r^2u^2v^2 + 1)^2}{4u^4} + \frac{B^2}{2},$$

$$(3.3) \quad \Delta_2 = \frac{1}{8u^6} (u^2(2Au + 2B - Cr^2v^2) - C) \left((2Au^3 - C) \times \left((-2Au^3 - 2Bu^2 + C)^2 + 3C^2r^4u^4v^4 \right) - 4Cr^2u^2v^2(Au^3 + C)^2 \right),$$

$$(3.4) \quad \Delta_3 = \frac{Cr^2(2Au^3 - C)(u^2(Cr^2v^2 - 2(Au + B)) + C)^4}{16u^8},$$

where we use the following notations:

$$u = \dot{\xi}/\dot{r}, \quad v = \dot{\varphi}/\dot{\xi}.$$

The thermodynamic stability in the free energy representation requires that the Hessian is a positive-definite symmetric $(0, 2)$ -tensor field. Accordingly, the minimal value of the free energy is ensured by the positiveness of the leading principal minors ($\Delta_k > 0$). In entropy representation, a system is thermodynamically stable if it satisfies the Second Law of Thermodynamics, namely, the entropy of the system reaches its maximum. Therefore, the indicatrices related to stable physical systems correspond to negative definite Hessians of Finsler-type Lagrangians (2.4).

The parameter v enters into the expression for minors (3.4) for even degree only. Consequently, the ranges of the space with the same signature, are symmetrical for positive and negative values $\dot{\varphi}/\dot{\xi}$. Let us analyze a sign of the minor Δ_1 , depending on parameters u . To do this, one can rewrite the minor Δ_1 in the form:

$$\Delta_1 = -\frac{3C^2(r^2u^2v^2 + 1)^2}{4u^4} - 6A^2u^2 - 6ABu - B^2.$$

Taking into account that A and C take positive values only, $\Delta_1 < 0$ at $B = 0$, and it changes its sign at $B < 0$ in the region of positive values of the parameter u ($u > 0$), or at $B > 0$ – in the region of negative value $u < 0$. For $u \rightarrow 0$, the main contribution is given by the term $-3C^2/(4u^4)$, $\Delta_1 < 0$. For $u \rightarrow \infty$, $\Delta_1 \rightarrow -6A^2u^2 < 0$, as well. Therefore, in the region $-\infty < u < \infty$, Δ_1 either does not change, or changes even times, its sign. Due to the complicated dependence of Δ_1 on u , to find analytically the solution of the equation $\Delta_1 = 0$ with respect to u , is a rather difficult problem. The equation $\Delta_1 = 0$ should be numerically solved. In fig. 3, the contour plots which separate the regions of positive and negative values of the minor Δ_1 , are shown for different values of the parameters u and v .

Now let us study the minor Δ_2 in the same way. For $u \rightarrow 0$, the main contribution is given by the term $C^3/(8u^6)$, so $\Delta_2 > 0$ at any values of the metric parameter A , B , C . For $u \rightarrow \infty$, we have $\Delta_2 \rightarrow 2A^4u^6 > 0$. Therefore, the minor Δ_2 does not change, or changes its sign even times, in the range of "u" $-\infty < u < \infty$. In fig. 3, the contour plots which separate the regions of positive and negative values of the minor Δ_2 , are presented for different values of u and v .

The sign of the minor $\Delta_3 = \text{Det}g_{ij}$ is defined by the sign of the multiplier $2Au^3 - C$: $\Delta_3 < 0$ for $2Au^3 - C < 0$, i.e., $u < \sqrt[3]{C/2A}$; vice versa, $\Delta_3 > 0$ for $2Au^3 - C > 0$ or for $u > \sqrt[3]{C/2A}$. Let us note that the sign of the minor Δ_3 does not depend on B and v . The contour plots for Δ_3 are shown in fig. 3. The regions I, ..., VI of values of the parameters (u, v) with different sets $\{\text{sign}(\Delta_1), \text{sign}(\Delta_2), \text{sign}(\Delta_3)\}$ at $B = 10, 10^{-15}, -10$, are presented in fig. 3. The signatures defined by the indexes of inertia (n_+, n_-) (we call them *the signatures of the Hessian*) which correspond to different regions (u, v) , are presented in Table 1. The regions I, II, and VI have the same Hessian signature (1,2), the regions III and V have the Hessian signature (2,1). The region IV holds the indexes of inertia (0, 3). When parameter B is close to zero or takes negative values, the space regions III and V holding at $B = 10$ are absent. But, for $B = -10$, the space region VI with $\{\text{sign}(\Delta_1), \text{sign}(\Delta_2), \text{sign}(\Delta_3)\} = \{+, -, +\}$ appears. Thus, there always exists a physically meaningful region of parameters (u, v) .

Since the Jacobi minors method does not allow to correlate a sign with definite space coordinates and, consequently, to find all the regions having different metric signatures, in order to study the metric signature we numerically calculated the eigenvalues and the corresponding eigenvectors of the metric tensor g_{ij} (2.7). The characteristic equation for eigenvalues λ , has the form:

$$(3.5) \quad \lambda^3 - \lambda^2 \text{tr}g + \lambda(\mathcal{A}_{11} + \mathcal{A}_{22} + \mathcal{A}_{33}) - \Delta_3 = 0$$

where $\text{tr}g = g_{11} + g_{22} + g_{33}$ is the trace of the metric tensor, and \mathcal{A}_{ij} are the algebraic complements defined by the expressions:

$$\mathcal{A}_{11} = g_{22}g_{33} - g_{23}^2, \mathcal{A}_{22} = g_{11}g_{33} - g_{13}^2, \mathcal{A}_{33} = g_{11}g_{22} - g_{12}^2.$$

For each eigenvalue, the corresponding eigenvector \mathbf{v}_i , $i = 1, \dots, 3$ is numerically calculated, according to the formula: $g\mathbf{v} = \lambda\mathbf{v}$. If the metric tensor is diagonal, then the eigenvectors are chosen as unit vectors along the axes ($\mathbf{v}_j^{(i)} = \delta_{ij}$). For the non-diagonal metric tensor, the eigenvectors are defined by the expression¹:

$$\mathbf{v}_i = \begin{pmatrix} \frac{\mathcal{A}_{11} + \lambda_i g_{11} + \lambda_i^2 - \lambda_i \text{tr}g}{\mathcal{A}_{13} + \lambda_i g_{13}} \\ \frac{\mathcal{A}_{12} + \lambda_i g_{12}}{\mathcal{A}_{13} + \lambda_i g_{13}} \\ 1 \end{pmatrix},$$

where the algebraic complements are

$$\mathcal{A}_{13} = g_{12}g_{23} - g_{13}g_{22}, \mathcal{A}_{12} = g_{13}g_{23} - g_{12}g_{33}.$$

The eigenvector was considered as a vector related coordinate t , r or φ , for the largest corresponding component. The sign of the eigenvalue corresponds to the sign of the metric signature for this coordinate.

In figs. 4 and 5, the results of numerical calculation of indicatrix regions corresponding to different metric signatures, are shown for various values of the parameter B . As one can see, there always exist regions with metric signature $(- - -)$. For large positive values of B , for example, $B = 1$ and for enough large particle velocities $\Delta r/\Delta t = 1/u$ ("u" in the range $(-0.0015; -10^{-6}) \& (0; 0.0015)$) the regions of the pseudo-Finsler space with signature $(- - -)$ (the configuration space of stable Langmuir monolayer) are absent, and an indicatrix space $(\Delta x, \Delta y)$ -projection can live only in regions with Hessian signature $(2, 1)$ or $(1, 2)$. It should be noted that the unified region with Hessian signature $(2, 1)$ – which has been determined by Jacobi minors method – is split into subregions with different metric signature $(+ + -)$, $(+ - +)$ and $(- + +)$. The decrease of B at phase transition leads to the emerging indicatrix regions with metric signature $(- - -)$, even for low particle velocities $\Delta r/\Delta t$ (for enough large values of u). The indicatrix part, placed in the space with metric signature $(- - -)$, increases with the decrease of B , as shown in fig. 5(a-f), for large Δt . When the metric parameter B tends to zero and takes further negative values, the space is characterized by the existence of regions with signatures $(- - +)$, $(+ - -)$, $(- + -)$, with the inertia index $(1, 2)$; and $(- - -)$, with the inertia index $(0, 3)$ only.

¹Here we take into account the symmetry of the metric tensor $g_{ij} = g_{ji}$.

If the lack of precision does not allow to separate the different signature space regions, then the Hessian signature $((1, 2))$ is only presented in simulation results. The space regions with Hessian signature $(1, 2)$ is placed near the singularity $\dot{r} = 0$. Numerical calculations show that the space region with signature $(+ - -)$ narrows at decrease of B , as one can see in the comparison within fig. 5(a-f).

In the spatial regions with signatures $(1, 2)$, the open trajectories are typical. From physical point of view, the space with signature $(1, 2)$ describes free molecules of the Langmuir monolayer in a state of two-dimensional (2D) liquid. The configuration space with signature $(- - -)$ defines a steady state of a particle at rest or limit-circle trajectories, so it characterizes the regions of the stable monolayer in a 2D-crystal state.

4 The Douglas and Weyl tensors and projectively flat configuration space of 1st-order phase transition

Let us consider the geometry of spatial hypersurfaces at a given pseudotime moment. To do this, one should assume that the time ξ passes at a constant rate $\dot{\xi} = const$. Then these hypersurfaces confine to

$$(4.1) \quad dl_F(\vec{r}, \dot{\xi}) = \left(A \frac{\dot{\xi}^2}{\dot{r}} + B\dot{\xi} - C \frac{(\dot{r}^2 + r^2 \dot{\phi}^2)}{2\dot{\xi}} \right) = \dot{\xi}.$$

If $\dot{\xi} \neq 0$ the choice is unambiguous. A number of the hypersurface satisfies the singular condition $\dot{\xi} = 0$. These hypersurfaces are

$$\dot{r}^2 + r^2 \dot{\phi}^2 = o(\dot{\xi}).$$

In the paper [5], we considered the pseudo-Finsler subspace of the statistical manifold with the metric function

$$(4.2) \quad F^2 = dl_F(\vec{r}, \dot{\xi})\dot{\xi},$$

which determines the system behavior on the hypersurface, subjected to the condition

$$(4.3) \quad mc^2 \dot{\xi} - L(s)\dot{\xi} = \dot{\xi} \rightarrow mc^2 - L(s) = 1$$

and therefore named a *mass surface*. The metric function (4.2) is the pseudo-Finsler metric function (2.4) out of the singularity at $\dot{\xi} \rightarrow 0$. The metric function (4.2) lives on the mass surface (4.3). The condition is equivalent to selecting the flow of time with constant rate $\dot{\xi} = 1$, or to considering of evolution parameter s as pseudo-time variable t : $t = s$. Since the condition (4.3) at $\dot{\xi} \rightarrow 0$ holds on any surface, in the general case of the Finsler metric function (2.4) there exist an arbitrariness of the mass-surface choice by means of the transformation (4.3) at $\dot{\xi} \rightarrow 0$. The mass surface is a space with a restricted geometry of paths.

We remove this arbitrariness by changing s into a new evolution parameter $T = T(s)$, such that the dependence on the variable $\xi = \xi(T)$ presents itself as a uniform flow of proper pseudo-time, i.e., $\frac{d\xi(T)}{dT}$ is constant. Then, in the singular area of the configuration space, we perform the following change of evolution parameter:

$$(4.4) \quad \frac{d\xi}{ds} = \frac{d\xi}{dT} \frac{dT}{ds} = \epsilon \frac{d\xi}{dT} \rightarrow 0, \quad \epsilon \rightarrow 0$$

which holds, because $\dot{\xi} \rightarrow 0$ lives in this region. Such changes of type (4.4) are named projective transformations. The projective transformation (4.4) of variables in the function (2.4) produces the following non-singular Finsler function in the singular region:

$$(4.5) \quad \bar{\mathcal{L}} = \frac{1}{\epsilon^2} \mathcal{L} = \frac{1}{\epsilon^2} dl_F^2 = - \left(A \frac{\xi_T^2}{r_T} + B \xi_T - \frac{C}{2} \frac{(r_T^2 + r^2 \varphi_T^2)}{\xi_T} \right)^2, \quad \epsilon \rightarrow 0.$$

Here the subindex T denotes the increment of variables $x = \{x^1, x^2, x^3\} \equiv \{\xi, r, \phi\}$ at the increase of T from T to $T + \Delta T$. The function (4.5) is a non-singular part of the metric function on the mass surface. Let us suppose that $T = T_{ph}$ is a proper-time moment of phase transition ending, with the relaxation time

$$(4.6) \quad \tau_{ph} = \frac{dT}{ds}, \quad T \neq T_{ph}$$

for the phase transition in the monolayer. The non-singular function (4.5) can be obtained by subtraction of a divergence in the form of the Dirac δ -function from the origin function, diverged at $T = T_{ph}$ as:

$$(4.7) \quad \mathcal{L} - A(x, x_T) \delta(T - T_{ph}) = dl_F^2 - A(x, x_T) \delta(T - T_{ph}) = - \left(A \frac{\xi_T^2}{r_T} + B \xi_T - \frac{C}{2} \frac{(r_T^2 + r^2 \varphi_T^2)}{\xi_T} \right)^2,$$

where $A(x, x_T)$ is the weight of the δ -function. Then, the metric function on the mass surface is

$$(4.8) \quad \mathcal{L} = dl_F^2 = - \left(A \frac{\xi_T^2}{r_T} + B \xi_T - \frac{C}{2} \frac{(r_T^2 + r^2 \varphi_T^2)}{\xi_T} \right)^2 + A(x, x_T) \delta(T - T_{ph}).$$

Thus, by using the function (4.8), we proved that the phase transition in the system with the proper life-time $\tau_{ph} = \xi$, evolves with an uniform flow of the proper pseudo-time $\xi = T$, and the behavior of the system becomes singular over the proper time at $T = T_{ph}$.

Let us construct a spray $\bar{G}^i(x, x_T)$, living on a mass surface. For the evolution (4.8) over the proper time, the velocity ξ , $\xi = T$ tends to zero at $T = T_{ph}$. Therefore, using (4.6), the projective transformation (4.4) can be extended to the whole configuration space (extended over the singular region), as

$$(4.9) \quad \frac{d\xi}{ds} = \frac{d\xi}{dT} \frac{dT}{ds} = \frac{d\xi}{dT} (1 - \Theta(\xi - T_{ph})) \tau_{ph} \rightarrow 0, \quad T \rightarrow T_{ph}.$$

After the change $s \rightarrow T$, the Euler-Lagrange equations (2.5) are transformed to

$$(4.10) \quad \left[\frac{d^2 x^i}{dT^2} + 2G^{(i)}(x, x_T) \right] \left(\frac{dT}{ds} \right)^2 = -x_T^i \frac{d^2 T}{ds^2}.$$

Therefore, taking into account (4.9), after performing the projective transformation,

the spray gets the following form:

$$(4.11) \quad \begin{aligned} \overline{G}^i(x, x_T) &= G^i(x, x_T) + \left(\frac{dT}{ds}\right)^{-2} x_T^i \frac{d^2T}{ds^2} = G^i(x, x_T) \\ &- \frac{1}{2} \delta(\xi - T_{ph}) x_T^i \xi_T (1 - \Theta(\xi - T_{ph}))^{-1} \equiv G^i(x, x_T) - \frac{1}{2} \delta(\xi - T_{ph}) x_T^i \xi_T. \end{aligned}$$

The divergence of Eq. (4.11) is stipulated by the singular scalar coefficient function

$$(4.12) \quad P = \delta(\xi - T_{ph}) \xi_T.$$

For the spray (4.11) considered for $T \rightarrow T_{ph}$, one gets $\frac{dx^1}{dT} = \int \delta(T - T_{ph}) dT \equiv 1$.

The projective transformations preserve the projective curvature tensor W_k^i :

$$(4.13) \quad W_k^i = H_k^i - H \delta_k^i - \frac{1}{n+1} \left(\frac{\partial H_k^j}{\partial \dot{x}^j} - \frac{\partial H}{\partial \dot{x}^k} \right) \dot{x}^i, \quad n = 3,$$

and the associated with it Weyl curvature tensor

$$(4.14) \quad W_{i\ kl}^j = \frac{1}{3} \left(\frac{\partial^2 W_k^j}{\partial \dot{x}^i \partial \dot{x}^l} - \frac{\partial^2 W_l^j}{\partial \dot{x}^i \partial \dot{x}^k} \right).$$

Here

$$(4.15) \quad H_k^i = 2 \frac{\partial G^i}{\partial x^k} - \frac{\partial^2 G^i}{\partial x^h \partial \dot{x}^k} \dot{x}^h + 2 G_k^i G^l - \frac{\partial G^i}{\partial x^l} \frac{\partial G^l}{\partial x^k}, \quad H = \frac{1}{n-1} H_i^i, \quad n = 3.$$

The projective transformations preserve the projective connection

$$(4.16) \quad \Pi_k^i{}^l = G_k^i G^l - \frac{1}{n+1} (\delta_l^i G_r^r{}^k + \delta_k^i G_r^r{}^l + \dot{x}^i G_r^r{}^l{}_k), \quad n = 3$$

and the associated with it tensor $B_{i\ kl}^j$ introduced by Douglas and defined through the derivatives of the projective connection coefficients $\Pi_k^i{}^l$:

$$(4.17) \quad B_{i\ kl}^j \equiv \frac{\partial \Pi_{i\ k}^j}{\partial x^l} = G_{i\ kl}^j - \frac{1}{n+1} (\delta_l^i G_r^r{}^k + \delta_k^i G_r^r{}^l + \dot{x}^i G_r^r{}^l{}_k), \quad n = 3.$$

Let us calculate the Douglas tensor at $\dot{\xi} = 0$. Since P (4.12) depends on the coordinate ξ of order one only, $\xi_T = 1$ and diverges, the tensor $\overline{G}_k^i{}^l$ is determined in the singular region as:

$$(4.18) \quad \overline{G}_k^i{}^l \Big|_{\dot{\xi} \rightarrow 0} \rightarrow - \frac{\partial P}{\partial x_T^k} \delta_l^i - \frac{\partial P}{\partial x_T^l} \delta_k^i - \frac{\partial^2 P}{\partial x_T^k \partial x_T^l} x_T^i \equiv 0.$$

By substituting (4.18) into (4.17), one immediately proves that the projective connection $B_{i\ kl}^j$ (4.17) vanishes:

$$(4.19) \quad B_{i\ kl}^j = 0.$$

Now we calculate the Weyl curvature tensor at $\dot{\xi} = 0$. The tensor \overline{H}_k^i obtained after applying the projective transformation Q of H_k^i is explicitly given as

$$(4.20) \quad \overline{H}_k^i = H_k^i + x_T^i \left[\left(\frac{\partial Q}{\partial x_T^k} \right)_{(h)} x_T^h - 2Q_{(k)} - Q \frac{\partial Q}{\partial x_T^k} \right] + \delta_k^i (Q_{(h)} x_T^h + Q^2).$$

Here the covariant derivatives $U_{(h)} = Q_{(h)}$, $\left(\frac{\partial Q}{\partial x_T^k} \right)_{(h)}$ are determined as

$$(4.21) \quad x_T^h U_{(h)} = \frac{\partial U}{\partial x^h} x_T^h - 2 \frac{\partial U}{\partial x_T^h} G^h$$

$$(4.22) \quad x_T^i U_{(k)} \equiv \sum_{l,m;l=m} \delta_l^i x_T^l \frac{\partial U}{\partial x^m} \delta_k^m - \frac{1}{2} \sum_{l,m;l=m} \delta_l^i x_T^l \frac{\partial U}{\partial x_T^j} \frac{\partial G^j}{\partial x_T^m} \delta_k^m = x_T^i \left(\frac{\partial U}{\partial x^k} - \frac{1}{2} \frac{\partial U}{\partial x_T^j} \frac{\partial G^j}{\partial x_T^k} \right),$$

and because considering the Euler theorem for homogeneous functions, G^i can be expressed as

$$2G^i = \frac{1}{2} \sum_k \frac{\partial G^i}{\partial x_T^k} x_T^k,$$

where $Q = P$ in our case. Since P (4.12) depends on the coordinate ξ of degree one only, $\xi_T = 1$ and diverges, the tensor \overline{H}_k^i is determined in the singular region as:

$$(4.23) \quad \overline{H}_k^i \Big|_{\dot{\xi} \rightarrow 0} \rightarrow -2x_T^i \frac{\partial P}{\partial x^k} + \delta_k^i \left(x_T^h \frac{\partial P}{\partial x^h} + P^2 \right).$$

By substituting (4.23) into (4.13), one immediately proves that the Weyl tensor $W_{i \ kl}^j$ (4.14) vanishes:

$$(4.24) \quad W_{i \ kl}^j = 0.$$

The known theorem reads (see [28, p. 183]) that the path space is projectively flat if the Weyl tensor $W_{i \ kl}^j$ and the projective connection $B_{i \ kl}^j$ both identically vanish. This means that there exists a flat space with a restricted path geometry in the configuration space at $\dot{\xi} \rightarrow 0$, endowed with the singular Finsler metric function (2.4). Accordingly, the configuration space is projectively flat.

Thus, the configuration space of 1st-order phase transition is projectively flat, as the Weyl $W_{i \ kl}^j$ and Douglas $B_{i \ kl}^j$ tensors identically vanish. The vanishing of the curvature tensor in the singular area certifies that the electrocapillary forces cease to act at the monolayer separation (emergence) from the subphase surface, when the phase transition is completed.

5 Discussion

Theorem 5.1. *In the configuration space of a monolayer in a state of the first-order phase transition, there always exists an indicatrix in space-pseudotime with the signature (0, 3).*

Proof. At small $\Delta t, \Delta x, \Delta y$ the indicatrix is not split, and is always located outside the region with sign-alternating signature, except of a very narrow region with signature $(1, 2)$, according to the comparison between spatial indicatrix sections (see fig. 4) for the indicatrices, which figs. 2b–h show. Meanwhile, the width of indicatrix region of sign-alternating signature $(1, 2)$ at $\Delta x, \Delta y \rightarrow 0$ trends to zero. At $\dot{\xi} = 0$, the indicatrix is an isotropic one, due to the vanishing of the Douglas and Weyl tensors (4.19, 4.24). Therefore the region with the signature $(1, 2)$ located at the cross-section of the indicatrix with a plane orthogonal to the axis Δt , shrinks to a point. This proves the claim. \square

Theorem 5.2. *In the configuration space of a monolayer being in a state of first order phase transition, there always exists a metastable state.*

Proof. The thermodynamically unstable state is characterized by the thermodynamic phase space, the space-pseudotime configurations, with regions having signatures different from $(0, 3)$. The minor Δ_3 turns out to be sign-alternating in the whole region of parameters (u, v) (see Table 2). Accordingly, there always exists a region of the space-pseudotime with signature different from $(0, 3)$. Several indicatrix evolutions are shown in fig. 5. Though at $dt \rightarrow 0$ the indicatrix which is transversal to the space-pseudotime region with the signature $(1, 2)$, is wholly located in the space with signature $(0, 3)$, it still evolves in the space with sign-alternating signature. In the process of evolution, one of its sheets touches the space-pseudotime plane with signature $(1, 2)$, which proves the claim. \square

Theorem 5.3. *The first-order phase transition in monolayers always corresponds to a change of the space-pseudotime signature.*

Proof. According to figs. 1f and h, the velocity $\dot{\xi}$ tends to zero and we have $B < 1$ in the 1st-order phase transition. At $\dot{\xi} \rightarrow 0$, the indicatrix transversal to space region of sign-alternating signature falls into a singularity, because the metric function (2.4) diverges: $dF(\dot{r}, \dot{\phi}, \dot{\xi}, \dots) \rightarrow \infty$ at $\dot{\xi} \rightarrow 0$. Meanwhile, if $B \leq 1$, after the splitting of the indicatrix, its non-closed part in spatial section is located in both space-pseudotime regions with signatures $(1, 2)$ and $(- - -)$ (see figs. 2b–h and fig. 4). Therefore, the state in the vicinity of singularity is a metastable one. When the singularity is not yet reached, the system stays in a metastable state. Therefore at the 1st-order phase transition, there always exists a metastable state with the signature $(1, 2)$, which proves the claim. \square

6 Conclusions

Based on the dynamics of monolayer in the contact statistical manifold and a performing the signature analysis of the appropriate space, one can conclude that the configurational space of the system is a projectively flat contact manifold. It was shown that the first-order phase transitions in Langmuir monolayers always occur with a change of signature of the given metric space. **Acknowledgements.** The present work was developed under the auspices of the Project BRFFR No. F20RA-007, within the cooperation framework between Romanian Academy and Belarusian Republican Foundation for Fundamental Research.

References

- [1] P. L. Antonelli, R. S. Ingarden, M. Matsumoto, *The Theory of Sprays and Finsler Spaces with Applications in Physics and Biology*, Fundamental Theories in Physics 58, Kluwer Academic Publ., 1993.
- [2] L. R. Arriaga et al., *Domain-growth kinetic origin of nonhorizontal phase coexistence plateaux in Langmuir monolayers: compression rigidity of a raft-like lipid distribution*, J. Phys. Chem. B 114 (2010), 4509-4520.
- [3] M. Avrami, *Kinetics of phase change*, J. Chem. Phys. 7 (1939) 1103; 8 (1940) 212; 9 (1941) 177.
- [4] V. Balan, H. Grushevskaya, N. Krylova, *Finsler geometry approach to thermodynamics of first order phase transitions in monolayers*, Diff. Geom. Dyn. Systems 17 (2015), 24-31.
- [5] V. Balan, H. V. Grushevskaya, N. G. Krylova, G. G. Krylov, I. V. Lipnevich, *Two-dimensional first-order phase transition as signature change event in contact statistical manifolds with Finsler metric*, Applied Sciences, 21 (2019), 11-26.
- [6] V. Balan, H. V. Grushevskaya, N. G. Krylova, M. Neagu, *Multiple-relaxation-time Finsler-Lagrange dynamics in a compressed Langmuir monolayer*, Int. J. Nonlinear Phenomena in Complex Systems, 19, 3 (2016), 223-253.
- [7] V. Balan, G. Grushevskaya, N. Krylova, M. Neagu, A. Oana, *On the Berwald-Lagrange scalar curvature in the structuring process of the LB-monolayer*, Applied Sciences, 15 (2013), 30-42.
- [8] A. Bravetti, C. S. Lopez-Monsalvo, F. Nettel, H. Quevedo, *Representation invariant Geometrothermodynamics: applications to ordinary thermodynamic systems*, J. Geom. Phys. 81 (2014), 1-9.
- [9] I. Bucataru, G. Cretu, *A characterization for Finsler metric of constant curvature and a Finslerian version of Beltrami theorem*, J. Geom. Analysis, 30 (2020), 617-631.
- [10] S. S. Chern, Z. Shen, *Riemann-Finsler Geometry*, World Scientific Publishing Co, Singapore, 2005.
- [11] U. Gehlert, D. Vollhardt, *Nonequilibrium structures in 1-monopalmitoyl-rac-glycerol monolayers*, Langmuir 13 (1997), 277.
- [12] M. Gheorghe, *The Indicatrix in Finsler Geometry*, An. St. Univ. "AL.I. Cuza" Iasi, (S.N.) Matematica, vol. LIII, Supliment, (2007), 163-180.
- [13] H. V. Grushevskaya, G. G. Krylov, N. G. Krylova, I. V. Lipnevich, *Modeling of the behavior and statistical analysis of compressibility in the process of Langmuir monolayer structurization*, J. Phys. CS, 643 (2015), 012015.
- [14] H. V. Grushevskaya, N. G. Krylova, *Effects of Finsler geometry in physics surface phenomena: case of monolayer systems*, H.N.G.P., 1 (15), 8 (2011), 128-146.
- [15] H. V. Grushevskaya, N. G. Krylova, *Phase transitions in geometrothermodynamic model of charged generalized-NUT black holes*, J. Phys. CS, 1557 (2020), 012024.
- [16] H. V. Grushevskaya, N. G. Krylova, I. V. Lipnevich, *Design and compressibility of Langmuir monolayers from organometallic nanocyclic complexes*, J. Phys. CS, 741 (1) (2016), 012116.
- [17] W. Johnson, R. F. Mehl, *Reaction kinetics in processes of nucleation and growth*, Trans. AIME. 135 (1939), 416.

- [18] N. G. Krylova, H. V. Grushevskaya, *Geometrical modeling of compressibility dynamics of the Langmuir monolayer*(in Russian), Proceedings of the National Academy of Sciences of Belarus, Physics and Mathematics Series, 54 (1) (2018), 84-96.
- [19] J. M. Lopez, M. J. Vogel, A. H. Hirs, *Influence of coexisting phases on the surface dilatational viscosity of Langmuir monolayers*, Phys. Rev. E, 70 (2004) 056308.
- [20] M. Matsumoto, *On the indicatrices of a Finsler space*, Periodica Mathematica Hungarica, 8, 2 (1977), 185-191.
- [21] J. Jr. Minones, P. Dynarowicz-Latka, R. Seoane, E. Iribarnegaray, M. Casas, *Brewster angle microscopy studies of the morphology in dipalmitoyl phosphatidyl glycerol monolayers spread on subphases of different pH*, Progr. Colloid Polym. Sci. 123 (2004) 160-163.
- [22] N. Nandi, D. Vollhardt, *Anomalous temperature dependence of domain shape in Langmuir monolayers: role of dipolar interaction*, J. Phys. Chem. B, 108 (2004), 18793.
- [23] M. Ostili, G. Bianconi, *Statistical mechanics of random geometric graphs: geometry-induced first-order phase transition*, Phys. Rev. E., 91 (2015), 042136.
- [24] P. Petersen, *Riemannian Geometry*(2nd ed.), Graduate Texts in Mathematics 171, Springer-Verlag, Berlin, New York, 2006.
- [25] E. Popovici, *On the volume of the indicatrix of a complex Finsler space*, Turkish Journal of Mathematics, 41, 2 (2017), 267-281.
- [26] H. Quevedo, *Geometrothermodynamics*, J. Math. Phys. 48 (2007), 013506.
- [27] P. Rashevski, *Polymetric geometry*, In: "Proceedings of Seminar on vector and tensor analysis with its applications into geometry and physics" , (Ed.: V. F. Kagan), Vol. 5, State Publishing Company of Technical and Theoretical Literature, Moscow, Leningrad, 1941, 21-147.
- [28] H. Rund, *Differential Geometry of Finsler Spaces*, Science Eds., Moscow, 1981.
- [29] G. Ruppeiner, *Thermodynamics: A Riemannian geometric model*, Phys. Rev. A 20 (1979), 1608.
- [30] D. Vollhardt, *Brewster angle microscopy: a preferential method for mesoscopic characterization of monolayers at the air/water interface*, Curr. Opinion in Colloid Interface Sci. 19, (3) (2014) 183-197.
- [31] D. Vollhardt, V. B. Fainerman, *Kinetics of two-dimensional phase transition of Langmuir monolayers*, J. Phys. Chem. B 106 (2002) 345-351.
- [32] D. Vollhardt, V. B. Fainerman, *Progress in characterization of Langmuir monolayers by consideration of compressibility*, Advances in Colloid and Interface Science, 127 (2006), 83-97.
- [33] F. Weinhold, *Metric geometry of equilibrium thermodynamics I, II, III, IV*, J. Chem. Phys. 63 (1975); 2479, 2484, 2488, 2496.
- [34] F. Weinhold, *Metric geometry of equilibrium thermodynamics V*, J. Chem. Phys. 65 (1976), 558.
- [35] M. Xiaohuan, *Weyl curvature of a Finsler space*, Appl. Math. J. Chinese Univ., Ser. B, 20 (1) (2005), 10-20.

Authors' addresses:

Halina Grushevskaya, George Krylov
Faculty of Physics, Belarusian State University, 4 Nezavisimosti Ave.,
220030 Minsk, The Republic of Belarus.
E-mail: grushevskaja@bsu.by, krylov@bsu.by

Nina Krylova
Faculty of Physics, Belarusian State University, 4 Nezavisimosti Ave.,
220030 Minsk, The Republic of Belarus;
Agropower Faculty, Belarusian State Agrarian Technical University,
99 Nezavisimosti Ave., 220023 Minsk, The Republic of Belarus.
E-mail: nina-kr@tut.by

Vladimir Balan
University Politehnica of Bucharest, Splaiul Independentei 313,
060042 Bucharest, Romania.
E-mail: vladimir.balan@upb.ro